



Evaluating the performance of the Inexact-Newton-Krylov scheme using globalization and forcing terms for non-Newtonian flows

Linda Gesenhues

linda@nacad.ufrj.br

José J. Camata

camata@nacad.ufrj.br

Alvaro L.G.A. Coutinho

alvaro@nacad.ufrj.br

High Performance Computing Center, Federal University of Rio de Janeiro

P.O. Box 68506, RJ 21945-970, Rio de Janeiro, Brazil

Abstract. *Non-Newtonian fluids are widely spread in industry. Examples are polymer processing, paint, food production or drilling muds. The dependence of the viscosity on the shear rate adds nonlinearity to the governing equations which complicates solving the transient, incompressible Navier-Stokes equation. Here, we use a semi-discrete stabilized finite element formulation for the governing equation. Often Newton-type algorithms are used to solve the resulting system of nonlinear equations at each time step. Those algorithms can converge rapidly from a good initial guess. However, it may appear that they are too expensive, since exact solutions of the linearized system are required for each iteration step. Therefore, the Inexact Newton-Krylov method (INK) is used to solve the linearized system of the Newton-scheme, reducing the computational effort. Hereby, the balance between the accuracy and the amount of effort per iteration is described by a tolerance, the so-called forcing term. Globalization strategies, like backtracking or trust region methods, are used to enhance the robustness of the INK algorithm. In this study the effects of a globalization strategy and several forcing terms of the Inexact-Newton-Krylov are evaluated. As a globalization strategy a backtracking method is applied. We compare four different forcing terms to verify which one has the best convergence. To do so, we simulate a Bingham fluid of a benchmark cavity and Taylor-Couette flow, both in three-dimensions, and analyze nonlinear and linear convergence effects. We compare the num-*

ber of linear iterations and CPU time. Results are analyzed and discussed aiming to establish guidelines for an effective INK utilization in practice.

Keywords: *Inexact Newton-Krylov, backtracking, non-Newtonian fluids, forcing terms*

1 INTRODUCTION

The computation of non-Newtonian fluid behavior is of high importance due to the great occurrence of this type of fluids in industrial processes, such as polymer melts, paint, coating etc., and nature, e.g., mud or lava flows. In non-Newtonian fluid behavior the dependence between shear rate and the viscosity is nonlinear, which complicates solving the governing equations. For further information about implementation of non-Newtonian fluid behavior refer to Crochet et al. (1984); Gartling (1992); Owens & Phillips (2002). Due to convection and equal order interpolation for the velocity and pressure fields instabilities in the Galerkin formulation may arise. To avoid that stabilization terms are added to the governing equations (Tezduyar, 1992).

The stabilized finite element formulation of the Navier-Stokes equation results in a set of nonlinear equations for each time step. Often Newton-type schemes are used to solve those nonlinear equations. As long as the initial guess is sufficiently good, the Newton-schemes converges fast (Dembo et al., 1982; Kelley, 1995). However, the Newton-scheme can be very costly for high numbers of unknowns, since it computes the exact solutions at each iteration step. Indeed, those exact solutions are not needed if the non linear iterates are far away from the solution. Therefore, Krylov methods are used to solve Newton's method linearized systems.

To solve the governing equations we use an Inexact Newton-Krylov method (INK) to reduce the computational costs which may arise due to the nonlinearities. This is a compromise between the accuracy and the computational effort spent for each iteration. Hereby, the factors like quality of the initial Newton step, robustness of the Jacobian evaluation and the right forcing term are playing a major role for its success (Kelley, 1995). The forcing term is also known as the tolerance for what we solve the linearized system of equations and has a high importance regarding the numerical performance of the method. A wrong choice of the forcing term can lead the method to successive oversolving. Methods stating on how to adaptively choose a forcing term can be found in An et al. (2007); Dembo et al. (1982); Eisenstat & Walker (1996); Gomes-Ruggiero et al. (2008); Papadrakakis & Balopoulos (1991). Those mechanisms are often based on the reduction of the Euclidean norm of the nonlinear residual. To do so, it is necessary to find out what level of accuracy is required to maintain a low CPU time.

A globalization strategy can be used to improve the robustness of the INK method, for instance, supporting algorithms which are leading to convergence of the solution despite the lack of a sufficient initial solution. In general, two different globalization strategies can be found in the literature: backtracking methods and trust-region methods. The backtracking method adapts the step size to a smaller one, if necessary, to preserve the decrease of the residual norm of the nonlinear system. A trust region method chooses the step size within a specified "trust region" to reduce the residual norm. For more information refer to Bodart et al. (2011); Elias et al. (2004); Dennis Jr. & Schnabel (1983); Eisenstat & Walker (1996); Pawlowski et al. (2006).

Elias et al. (2006a) analyze INK performance, comparing the inexact Newton method, an inexact mixed method and classical methods for viscoplastic fluids. It is shown that the inexact Newton method is faster than the classical method for computing non-Newtonian fluid behavior. However, globalization strategies and forcing terms are not evaluated.

In this study we analyze the characteristics of forcing terms and globalization strategy behavior for non-Newtonian flows. We compare four different forcing terms to verify which one has the best convergence. First, a 3D benchmark cavity flow is computed using the different

forcing terms and a backtracking methods for a Bingham fluid. Later, we analyze the forcing terms by simulating a 3D Taylor-Couette flow using a Power Law and a Bingham fluid model. Non-linear and linear convergence effects are illustrated by the number of linear iteration steps and the CPU time. Results are analyzed and discussed aiming to establish guidelines for an effective INK utilization, regarding non-Newtonian fluid behavior in practice.

Therefore, we state the governing equations and the finite element formulation in Section 2.1 and 2.2. The INK method is discussed in Section 2.3. The used forcing terms are described in Section 2.4 and the backtracking is shown in Section 2.5. Section 3 contains the numerical results. In the end, Section 4 gives a summary of the results and our final recommendations.

2 METHODS

2.1 Governing and constitutive equations

On a spatial domain $\Omega \subset R^3$, with a piecewise regular surface and time interval $[0, t_f]$, an incompressible and viscous fluid in this region is governed by the Navier-Stokes equation:

$$\rho \left(\frac{\partial \mathbf{u}}{\partial t} + \mathbf{u} \cdot \nabla \mathbf{u} \right) - \nabla \cdot \boldsymbol{\sigma} = \mathbf{f} \quad \text{on } \Omega \times (0, t_f), \quad (1)$$

$$\nabla \cdot \mathbf{u} = 0 \quad \text{on } \Omega \times (0, t_f), \quad (2)$$

where \mathbf{u} represents the velocity field, ρ is the fluid density, $\boldsymbol{\sigma}$ is the stress tensor and \mathbf{f} is the body force.

The Dirichlet and natural boundary conditions are described by complementary subsets Γ_1 and Γ_2 of the boundary Γ :

$$\mathbf{u} = \mathbf{g} \quad \text{on } \Gamma_1, \quad (3)$$

$$\mathbf{n} \cdot \boldsymbol{\sigma} = h \quad \text{on } \Gamma_2. \quad (4)$$

The stress tensor $\boldsymbol{\sigma}$ can be described by:

$$\boldsymbol{\sigma}(p, \mathbf{u}) = -p\mathbf{I} + \mathbf{T}, \quad (5)$$

where \mathbf{I} is the identity tensor, p the hydrostatic pressure and \mathbf{T} is the deviatoric part of the stress tensor and can be stated as:

$$\mathbf{T} = 2\mu\boldsymbol{\varepsilon}(\mathbf{u}), \quad (6)$$

μ describes the dynamic viscosity, and $\boldsymbol{\varepsilon}$ the strain rate tensor, which is defined as:

$$\boldsymbol{\varepsilon} = \frac{1}{2}(\nabla \mathbf{u} + \nabla^T \mathbf{u}). \quad (7)$$

For a Newtonian fluid, the relationship between the stress tensor $\boldsymbol{\sigma}$ and the rate of strain $\boldsymbol{\varepsilon}$ is proportional. Thus, the dynamic viscosity μ is a constant.

The viscosity of a non-Newtonian fluid is dependent on other flow parameters, e.g. the deformation rate. So that Eq. 6 changes to:

$$\mathbf{T} = 2\mu(\dot{\gamma})\boldsymbol{\varepsilon}(\mathbf{u}), \quad (8)$$

where $\dot{\gamma}$ is the second invariant of the strain rate tensor and $\mu(\dot{\gamma})$ is the, so-called, apparent viscosity.

We consider two different kinds of non-Newtonian fluids in this work: a Bingham fluid and a Power Law fluid. More details about the rheology models can be seen in Crochet et al. (1984); Gartling (1992); Owens & Phillips (2002). A Power Law fluid can be described as follows:

$$\mu(\dot{\gamma}) = \begin{cases} \mu_0 K \dot{\gamma}^{n-1} & \text{if } \dot{\gamma} > \dot{\gamma}_0, \\ \mu_0 K \dot{\gamma}_0^{n-1} & \text{if } \dot{\gamma} \leq \dot{\gamma}_0, \end{cases} \quad (9)$$

where μ_0 is a nominal viscosity, K describes the consistency index, n is the power law parameter and $\dot{\gamma}_0$ is the cut off value for the second invariant of the strain rate tensor.

For the Bingham fluid a bi-viscosity model is used and is stated as:

$$\mu(\dot{\gamma}) = \begin{cases} \mu_0 + \frac{\sigma_Y}{\dot{\gamma}} & \text{if } \dot{\gamma} > \frac{\sigma_Y}{\mu_r - \mu_0}, \\ \mu_r & \text{if } \dot{\gamma} \leq \frac{\sigma_Y}{\mu_r - \mu_0}, \end{cases} \quad (10)$$

where σ_Y denotes the yield stress and μ_r describes the Newtonian viscosity, which is typically chosen to be approximately $100\mu_0$ to represent a Bingham fluid (Beverly & Tanner, 1992).

2.2 Finite element formulation

A semi-discrete finite element method is used to approximate the problem. According to Tezduyar et al. (1996) the function spaces are defined for the velocity and pressure as \mathbf{S}_u^h , \mathbf{V}_u^h , \mathbf{S}_p^h and $\mathbf{V}_p^h = \mathbf{S}_p^h$. According to Tezduyar & Osawa (2000) the SUPG/PSPG stabilized semi-discrete formulation of the incompressible Navier-Stokes Eqs. (1) and (2) can be written as: find $\mathbf{u}^h \in \mathbf{S}_u^h$ and $p^h \in \mathbf{V}_u^h$ such that $\forall \mathbf{w}^h \in \mathbf{V}_u^h$ and $\forall q^h \in \mathbf{V}_p^h$, where \mathbf{S}_u^h and \mathbf{S}_p^h are defined as:

$$\mathbf{S}_u^h = \{\mathbf{u}^h | \mathbf{u}^h(\cdot, t) \in (H^1(\Omega))^{nsd}, u^h = g \text{ on } \Gamma_1\}, \quad (11)$$

$$\mathbf{S}_p^h = \{p^h | p^h(\cdot) \in L^2(\Omega), \int_{\Omega} p^h d\Omega = 0 \text{ on } \Omega\}. \quad (12)$$

Here $(H^1(\Omega))^{nsd}$ describes the vector-valued functions space and $L^2(\Omega)$ denotes the scalar-valued functions space.

In Eq. (13) the first four integrals on the left side represent the Galerkin formulation. The other integral terms are additional terms for the stabilization of the finite element formulation. The stabilization terms hinder the spurious node-to-node oscillation of the velocity and pressure distribution. The first summation is the SUPG term, the second corresponds to the PSPG term and the last summation defines the least-squares incompressibility constraint (LSIC) term to prevent oscillation in high Reynolds number flows (Tezduyar, 2001). Hereby, the stabilization terms are evaluated as the sum of element-wise integral expression, where n_{el} is the number of elements in the mesh. The SUPG and PSPG stabilization parameters are chosen according to Tezduyar et al. (1991).

$$\begin{aligned}
 \int_{\Omega} \mathbf{w}^h \cdot \rho \left(\frac{\partial \mathbf{u}^h}{\partial t} + (\mathbf{u}^h \cdot \nabla) \mathbf{u}^h - \mathbf{f} \right) d\Omega + \int_{\Omega} \epsilon(\mathbf{w}^h) : \sigma(p^h, \mathbf{u}^h) d\Omega - \int_{\Gamma_2} \mathbf{w}^h \cdot \mathbf{h} d\Gamma_2 \\
 + \int_{\Omega} q^h \nabla \cdot \mathbf{u}^h d\Omega \\
 + \sum_{e=1}^{n_{el}} \int_{\Omega^e} \frac{1}{\rho} (\tau_{SUPG} \rho \mathbf{u}^h \cdot \nabla \mathbf{w}^h + \tau_{PSPG} \nabla q^h) \\
 \cdot \left[\rho \left(\frac{\partial \mathbf{u}^h}{\partial t} + \mathbf{u}^h \cdot \nabla \mathbf{u}^h \right) - \nabla \cdot \sigma(p^h, \mathbf{u}^h) - \rho \mathbf{f} \right] d\Omega \\
 + \sum_{e=1}^{n_{el}} \int_{\Omega^e} \tau_{LSIC} \nabla \cdot \mathbf{w}^h \rho \nabla \cdot \mathbf{u}^h d\Omega = \mathbf{0} \quad (13)
 \end{aligned}$$

The spatial discretization of Eq. (13) leads to a system of nonlinear ordinary differential equations as follows:

$$\mathbf{M} \dot{\mathbf{u}} + \mathbf{M}_{\delta}(\mathbf{u}) \dot{\mathbf{u}} + \mathbf{N}(\mathbf{u}) + \mathbf{N}_{\delta}(\mathbf{u}) + \mathbf{K} \mathbf{u} - (\mathbf{G} + \mathbf{G}_{\delta}) \mathbf{p} = \mathbf{f}_{\mathbf{u}}, \quad (14)$$

$$\mathbf{M}_{\varphi}(\mathbf{u}) \dot{\mathbf{u}} + \mathbf{G}^T \mathbf{u} + \mathbf{N}_{\varphi}(\mathbf{u}) + \mathbf{G}_{\varphi} \mathbf{p} = \mathbf{f}_{\mathbf{p}}, \quad (15)$$

where \mathbf{u} describes the vector of unknown nodal values of \mathbf{u}^h , \mathbf{p} is the vector of unknown nodal values of p^h and the superimposed dot implies time differentiation. The nonlinear vectors $\mathbf{N}(\mathbf{u})$, $\mathbf{N}_{\delta}(\mathbf{u})$, $\mathbf{N}_{\varphi}(\mathbf{u})$, and the matrices \mathbf{M} , $\mathbf{M}_{\delta}(\mathbf{u})$, $\mathbf{M}_{\varphi}(\mathbf{u})$, \mathbf{K} , \mathbf{G} , \mathbf{G}_{δ} , \mathbf{G}_{φ} originate from the temporal, convective, viscous and pressure terms. The vector $\mathbf{f}_{\mathbf{u}}$ contains the boundary conditions, the vector \mathbf{f} , the body force q and also the stabilization terms of all equations. The vector $\mathbf{f}_{\mathbf{p}}$ also includes boundary conditions and stabilization terms. The subscripts δ and φ identify the SUPG and PSPG contributions.

The system of Eqs. (14) and (15) are advanced in time by a fully coupled scheme. The discretization in time of the semi-discrete Eqs. (14) and (15) is accomplished by a predictor multicorrector finite difference scheme according to Franca & Frey (1992) and Hughes & Tezduyar (1984). For each time step, after linearization, we arrive at a nonlinear set of equations to be solved, which can be written independently from the time step as:

$$\mathbf{F}(\mathbf{x}) = \mathbf{0}, \quad (16)$$

where $\mathbf{x} = (\mathbf{u}, \mathbf{p})$ describes a vector of nodal unknowns. In Eq. (14) the approximate Jacobian form used is based on Taylor's expansions of the nonlinear terms. The approximate Jacobian form is described by Tezduyar (1999) and used in Elias et al. (2006b).

2.3 Inexact Newton-Krylov method

The Newton's method can be used to solve the nonlinear system of Eqs. (16). Newton's method approximates iteratively the function \mathbf{F} at a given point $\mathbf{x} = (x_1, x_3, \dots, x_N)^t$ by a linear function. Here, the Jacobian matrix \mathbf{J} describes the variation of the function \mathbf{F} regarding \mathbf{x} . For each iteration, Newton's method can be stated by:

$$\mathbf{x}^{k+1} = \mathbf{x}^k + \mathbf{s}^k, \quad (17)$$

where \mathbf{s}^k , the so-called inexact Newton step, is obtained by solving the linear system:

$$\mathbf{J}(\mathbf{x}^k)\mathbf{s}^k = -\mathbf{F}(\mathbf{x}^k). \quad (18)$$

The iteration stops when the relative nonlinear residual $\|\mathbf{F}(\mathbf{x}^k)\|_2/\|\mathbf{F}(\mathbf{x}^0)\|_2$ is small, i.e. when $\|\mathbf{F}(\mathbf{x}^k)\|_2 < \tau_{NL} = \tau_{res}\|\mathbf{F}(\mathbf{x}^0)\|_2$, for a given tolerance τ_{res} .

The Inexact Newton-Krylov (INK) method solves the system (18) iteratively. This is especially advantageous for large scale problems (Bellavia & Berrone, 2007; Pawlowski et al., 2006; Tuminaro et al., 2002; Elias et al., 2004; Rudi et al., 2015). It is also used to improve the computational performance by reducing precision. Thus, the balance between the accuracy and the amount of effort per iteration is controlled by a tolerance, the forcing term, expressed by η_k . The forcing term represents the tolerance of the inner iterative Krylov solver on the nonlinear iteration k , here we use GMRES as the Krylov solver. In Section 2.4 several forcing terms are introduced. The updated solution can be improved by \mathbf{x}^{k+1} on Eq. (17), if we consider $\mathbf{x}^{k+1} = \mathbf{x}^k + \lambda\mathbf{s}^k$, where $\lambda > 0$ is an appropriate parameter. In Section 2.5 a globalization method, the so-called backtracking, is described to calculate λ . This shortens the iteration steps if needed to ensure a eventually decrease in the nonlinear residual residual norm (Kelley, 1995).

2.4 Forcing terms

We denote the given maximum initial tolerance for the Inexact Newton method η_0 . The forcing term introduced by Papadrakakis & Balopoulos (1991), can be written as:

$$\eta_k^{PP} = \min\left\{\eta_0, \left(\frac{\|\mathbf{F}(\mathbf{x}^k)\|_2}{\|\mathbf{F}(\mathbf{x}^{k-1})\|_2}\right)^v\right\}, \quad (19)$$

where η_0 is a given maximum initial tolerance for the Inexact Newton method. The parameter v has the value of $v = 2$.

A new forcing term was introduced by Eisenstat & Walker (1996), also described by Kelley (1995).

$$\eta_k^A = \gamma \left(\frac{\|\mathbf{F}(\mathbf{x}^k)\|_2}{\|\mathbf{F}(\mathbf{x}^{k-1})\|_2}\right)^\alpha, \quad (20)$$

where γ and α are given parameters. The forcing term is written as:

$$\eta_k^{EW*} = \begin{cases} \eta_0 & k = 0, \\ \min\{\eta_0, \eta_k^A\} & k > 0. \end{cases} \quad (21)$$

To avoid that η_k^{EW*} is small for one or more iteration while \mathbf{x}^k is still far from the solution Eisenstat & Walker (1996) suggest a method with the idea that if η_{k-1}^{EW*} is sufficiently large, η_k^{EW*} cannot decrease by much more than a factor of η_{k-1}^{EW*} , that is

$$\eta_k^{EW*} = \begin{cases} \eta_0 & k = 0, \\ \min\{\eta_0, \eta_k^A\} & k > 0, \gamma(\eta_{k-1}^{EW*})^\alpha < \beta, \\ \min\{\eta_0, \max\{\eta_k^A, \gamma(\eta_{k-1}^{EW*})^\alpha\}\} & k > 0, \gamma(\eta_{k-1}^{EW*})^\alpha > \beta. \end{cases} \quad (22)$$

In the following two forcing terms are based on Eq. (22). One introduced by Kelley (1995), here called η_k^{EWK} , which considers $\alpha = 2$, $\gamma = 0.9$ and $\beta = 0.1$. The second is stated in the PETSc Library (Balay et al., 2016), here called η_k^{EWC} and considers $\alpha = \frac{1 + \sqrt{5}}{2}$, $\gamma = 1.0$ and $\beta = 0$. Note that both parameters in *EWC* and *EWK* were previously introduced optionally by Eisenstat & Walker (1996).

Furthermore, Gomes-Ruggiero et al. (2008) introduced a new definition of the forcing term depending on the change in $\|\mathbf{F}(\mathbf{x}^k)\|$ and the computational cost during the k th nonlinear iteration step, including inner iterations. The cost (price_k) is stated as the number of iterations performed by the linear solver (iter_k) plus the number of function evaluations (feval_k), that is, $\text{price}_k = \text{iter}_k + \text{feval}_k$. Both, iter_k and feval_k , contain the total number of inner iterations and the total number of function evaluations performed during the first k nonlinear iterations.

They also described a way to control the angle of the decrease of $\|\mathbf{F}\|$. Here, if θ_k is the slope coefficient of the iteration k of $\|\mathbf{F}\|$, $\cos(\theta_k)$ is used as a measure for the trade off between convergence and computational costs and can be described as the ratio:

$$\cos(\theta_k) = \frac{b_k}{\sqrt{a_k^2 + b_k^2}}, \quad (23)$$

where

$$\begin{aligned} a_k &= (\log_{10}\|\mathbf{F}(\mathbf{x}^k)\|_2 - \log_{10}\|\mathbf{F}(\mathbf{x}^{k-1})\|_2), \\ b_k &= \log_{10}(\text{price}_k - \text{price}_{k-1}), \end{aligned} \quad (24)$$

where $\theta \in (-\pi/2, \pi/2)$. If $\cos(\theta_k)$ is approaching -1 the procedure works well and a stricter forcing term may be applied. If $\cos(\theta_k)$ is close to zero, the iterations are either too costly or are leading nowhere (oversolving) and the forcing term has to be loosened. If $\cos(\theta_k)$ is positive, $\|\mathbf{F}(\mathbf{x}^k)\|$ has actually increased which has to be followed by a drastic action. Let

$$\eta_k^A = \left(\frac{1}{k+1}\right)^\nu [\cos(\theta_k)]^2 \left(\frac{\|\mathbf{F}(\mathbf{x}^k)\|_2}{\|\mathbf{F}(\mathbf{x}^{k-1})\|_2}\right), \quad (25)$$

where $\nu \in (1, 2]$ and is adopted by $\nu = 1.1$. In this study this forcing term is called *GLT* and is defined by:

$$\eta_k^{GLT} = \begin{cases} \eta_0 & k = 0, \\ \min\{\eta_0, \eta_k^A\} & k > 0. \end{cases} \quad (26)$$

It may happen that the final iterate will decrease $\|\mathbf{F}(\mathbf{x}^k)\|$ way more than desired and therefore, the cost of the last step is higher than necessary (Kelley, 1995). This is called oversolving and can be controlled by the comparison of the current nonlinear residual norm and the nonlinear norm where the iteration would terminate (τ_{NL}) and limit η_k^* by a constant multiple of $\tau_{NL}/\|\mathbf{F}(\mathbf{x}^k)\|$, stated as

$$\eta_k^* = \min\{\eta_0, \max\{\eta_k^*, \epsilon \tau_{NL}/\|\mathbf{F}(\mathbf{x}^k)\|_2\}\}. \quad (27)$$

In this study we consider $\epsilon = 0.5$ and the super index $*$ can be *PP*, *EWK*, *EWC* and *GLT*. Here, those four forcing terms are used to choose adaptively tolerances for the inner iterative method in each Inexact Newton iteration.

2.5 Backtracking

Backtracking is a globalization strategy used to enhance the robustness of the INK method. For a given inexact Newton step \mathbf{s}^k we define a step in this direction with an acceptable \mathbf{x}^{k+1} , by:

- (i) calculate a inexact Newton step \mathbf{s}^k ;
 - (ii) set $\mathbf{x}^{k+1} = \mathbf{x}^k + \lambda \mathbf{s}^k$ for $\lambda > 0$ so that \mathbf{x}^{k+1} is an acceptable next iterate.
- (28)

The backtracking strategy is also known as a line search method to choose λ in Eq. (28) minimizing a functional $f(\cdot)$. An example could be a problem-specific objective function or guarantee the progress of the residual minimization, in case a numerical solution of nonlinear partial differential equations is needed. Therefore: $f(\mathbf{x}) = \frac{1}{2} \mathbf{F}(\mathbf{x})^T \mathbf{F}(\mathbf{x})$.

In this study the backtracking strategy introduced by Dennis Jr. & Schnabel (1983) is used to solve the nonlinear Eq. (16). The Wolfe rule is applied, which reduces the integrate only if the following condition is satisfied:

$$f(\mathbf{x}^{k+1}) \leq f(\mathbf{x}) + \omega \lambda \nabla f(\mathbf{x})^T \mathbf{s}^k, \quad (29)$$

where $\omega \in (0, 1)$ and $\nabla f(\mathbf{x})^T \mathbf{s}^k$ describes the slope of $f(\mathbf{x})$ in the direction of \mathbf{s}^k . Here, we use $\omega = 10^{-4}$, according to Kelley (1995). The parameter λ is determined in order to produce a reduction such that $\sigma_0 \lambda_{old} \leq \lambda_{new} \leq \sigma_1 \lambda_{old}$, where $0 < \sigma_0 < \sigma_1 < 1$. The inexact Newton step \mathbf{s}^k is derived from Eq. 29 if $\nabla f(\mathbf{x})^T \mathbf{s}^k < 0$, where

$$\nabla f(\mathbf{x}) = \frac{d}{dx} \sum_{i=1}^n \frac{1}{2} (f_i(\mathbf{x}))^2 = \sum_{i=1}^n \nabla f_i(\mathbf{x}) f_i(\mathbf{x}) = \mathbf{J}(\mathbf{x})^T \mathbf{F}(\mathbf{x}). \quad (30)$$

Actually, the Newton direction along $\mathbf{s}^k = -\mathbf{J}(\mathbf{x})^{-1} \mathbf{F}(\mathbf{x})$ is a descent direction, since

$$\nabla f(\mathbf{x})^T \mathbf{s}^k = \mathbf{F}(\mathbf{x})^T \mathbf{J}(\mathbf{x}) (-\mathbf{J}(\mathbf{x})^{-1} \mathbf{F}(\mathbf{x})) = -\mathbf{F}(\mathbf{x})^T \mathbf{F}(\mathbf{x}) < 0. \quad (31)$$

3 NUMERICAL SIMULATION

In this section two benchmark problems are solved and analyzed, regarding their performance for a globalization strategy and several forcing terms. Here, we consider a Power Law fluid and a Bingham fluid. For all computations an Intel(R) Xeon(R) CPU E5-1620 v2 @370GHz with 4 cores and 8 GB memory running Linux Mint 17 is used. GNU is used as compiler with the optimization level 01.

In all experiments an edge-based nodal-block diagonal preconditioned GMRES solver with 35 vectors to restart (GMRES(35)) is used and the maximum number of allowed nonlinear iterations per time step is 8. We use a relative residuum tolerance of 0.001 and an inexact Newton step tolerance of 0.001. For the backtracking a maximum iteration number of 5 is used and a Newton tolerance of 10^{-4} for the Navier-Stokes equation. The maximum initial tolerance is $\eta_0 = 0.1$.

3.1 3D lid-driven cavity

A lid-driven cavity is used to analyze the performance of the different forcing terms. The benchmark cavity is a common tool to evaluate fluid flows. The domain and boundary conditions used in the simulation can be seen in Fig. 1. The walls at the bottom and in x -direction have a no slip boundary condition. The walls in y -direction have symmetry conditions. And the top lid has a dimensionless speed of 1.

The mesh is unstructured with linear tetrahedra and has 673914 elements, as well as, 128721 nodes. For the Bingham fluid, a dimensionless nominal viscosity of $\mu_0 = 1$ is chosen and therefore, a Newtonian viscosity of $\mu_r = 100$ is assumed. Taking into account the nominal viscosity, the Reynolds number is 1. The experiments were done for a final time of 0.25 s with a fixed time step of $\Delta t = 0.001$.

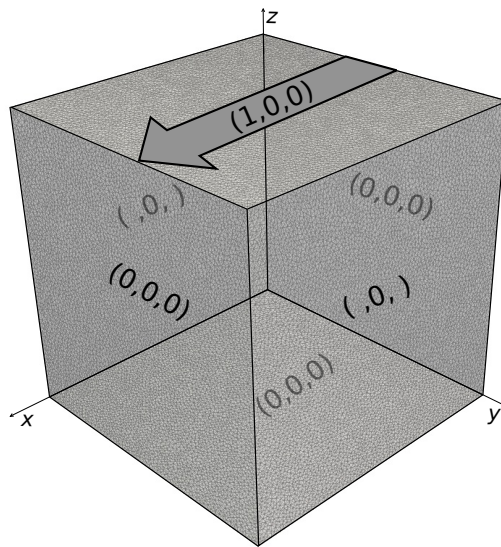


Figure 1: Geometry and boundary conditions of the benchmark cavity.

Figure 2 shows the velocity streamlines and the viscosity of the cavity y -plane using the EWC forcing term with backtracking. In areas with higher shear rates the viscosity is low. This is especially the case in the lower edges and in the middle, where a vortex eye can be found. Other regions are highly viscous, where the shear rate is not exceeding the threshold value and thus, a rigid zone is created.

To validate our model we compare the position of the vortex eye with former studies. In our simulation the z -coordinate of the vortex eye is approximately 0.7805, using a threshold of $\sigma_Y = 10$. The results agree well with the computations of Elias et al. (2006b); Vola et al. (2003); Mitsoulis & Zisis (2001).

In the following we analyze the performance of the benchmark cavity simulation. Here, we compare the sum of different parameters over a fixed simulation time of 0.25s. After this time the solution reaches steady-state. We also evaluate the total number of nonlinear iteration steps ($\sum iter$), the number of linear iterations ($\sum NLI$), the line search steps ($\sum LSS$), the line search rejected steps ($\sum LSR$) and the needed CPU time ($CPUtime$).

Table 1 shows the performance for the four different forcing terms with no backtracking. The most efficient one is the EWC, having the least number of linear iterations (89341) and the

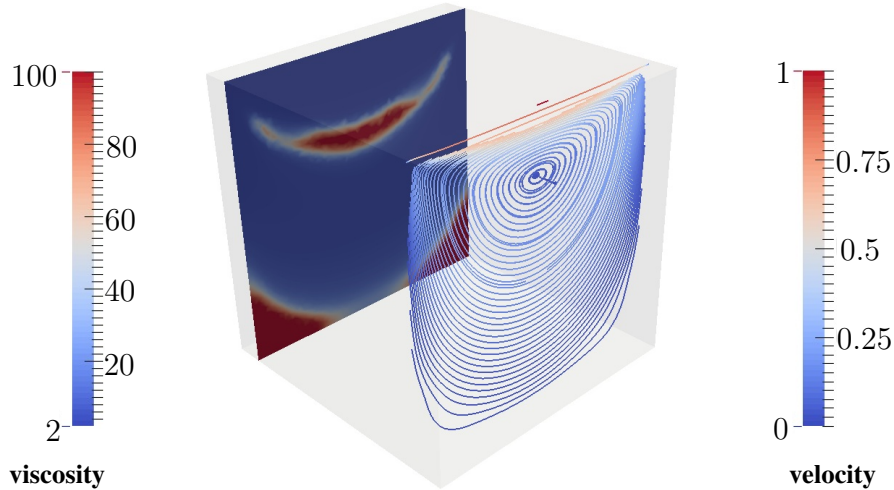


Figure 2: Viscosity and velocity streamlines of the benchmark cavity

lowest CPU time (92749 s). The second best performing forcing term is the GLT with 92138 linear iterations and a CPU time of 9582 s. The total number of nonlinear iteration steps for all forcing terms is constant and the sums of the line search steps and the line search rejected steps are zero, since the backtracking method is not used.

Table 1: Performance of the cavity simulating a Bingham fluid for different forcing terms, without backtracking

Forcing term	$\sum iter$	$\sum NLI$	$\sum LSS$	$\sum LSR$	$CPUtime$
EWC	2000	89341	0	0	9249
EWK	2000	96729	0	0	9665
GLT	2000	92138	0	0	9582
PP	2000	96498	0	0	9707

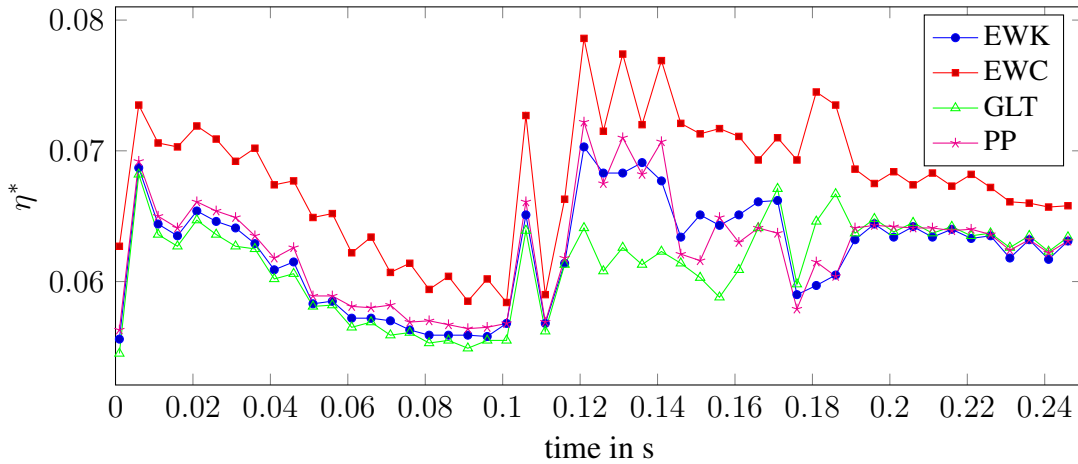
In Table 2 the characteristic values for the performance of the forcing terms of the cavity using the backtracking strategy are shown. For all cases the total number of nonlinear iteration steps and CPU time is lower. Here, the GLT forcing term shows the best characteristics with a total number of nonlinear iterations of 1806 and a CPU time of 8722 s. The second best performance shows the PP forcing term. However, the performance results of the different forcing terms are close together. Therefore, a clear statement cannot be made.

In Fig. 3 the average of the tolerances of the nonlinear solutions for each time step along the computation is shown. For the first hundred time steps the tolerances are decreasing. After, some oscillations can be seen. This may occur due to reaching the steady state.

The choice of the forcing term depends on the globalization strategy. In case of the benchmark cavity simulating a Bingham fluid the EWC and PP forcing terms are advantageous when backtracking is turned off. Using the backtracking strategy the GLT and PP forcing terms show the better performance. In general, computing time and number of needed iterations decreases when the backtracking method is used. The backtracking strategy is clearly improving the per-

Table 2: Performance of the cavity simulating a Bingham fluid for different forcing terms, with backtracking

Forcing term	$\sum iter$	$\sum NLI$	$\sum LSS$	$\sum LSR$	$CPUtime$
EWC	1867	82069	795	109	8959
EWK	1829	80477	790	108	8825
GLT	1806	80266	790	108	8722
PP	1828	80875	790	108	8819

**Figure 3: Average forcing term per time step simulating a Power Law fluid of the cavity flow, with backtracking**

formance.

3.2 3D Taylor-Couette flow

As a second test case a benchmark Taylor-Couette flow is computed. Thus, a viscous fluid between two rotating cylinders is analyzed. This is a popular test case because it can be easily evaluated doing experiments and compare those to analytical and numerical results. Especially, when it comes to validation of a model the Taylor-Couette flow is favorable. We analyze the computing performance of the forcing terms for a Bingham and a Power Law fluid.

The Taylor-Couette flow has an outer cylinder which has a non-dimensional radius of 1. The inner cylinder has a radius of 0.5. The geometry and boundary conditions are illustrated in Fig. 4. The inner cylinder is rotating at an angular velocity of 1. The outer cylinder is fixed with a no slip boundary condition. The bottom and the top have symmetry boundary conditions.

The mesh is composed by linear tetrahedra and has 74765 elements and 20946 nodes. The experiments were done for a final time of 0.8 s with a fixed time step of $\Delta t = 0.001$.

For the Bingham fluid a nominal viscosity of $\mu_0 = 1$ is chosen and, therefore, a Newtonian viscosity of $\mu_r = 100$ is assumed. The yield stress is $\sigma_Y = 10$. The Reynolds number is 1 using the nominal viscosity as the characteristic viscosity.

Figure 5a shows the velocity distribution in a z -plane of the Taylor-Couette flow using the EWC forcing term with backtracking. The velocity of the fluid decreases from the inner to the

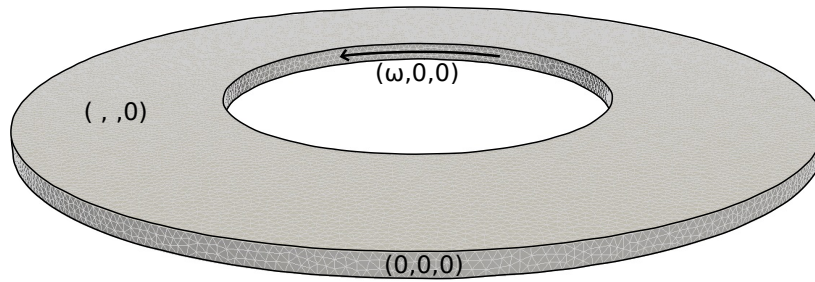


Figure 4: Geometry and boundary conditions of the benchmark Taylor-Couette flow.

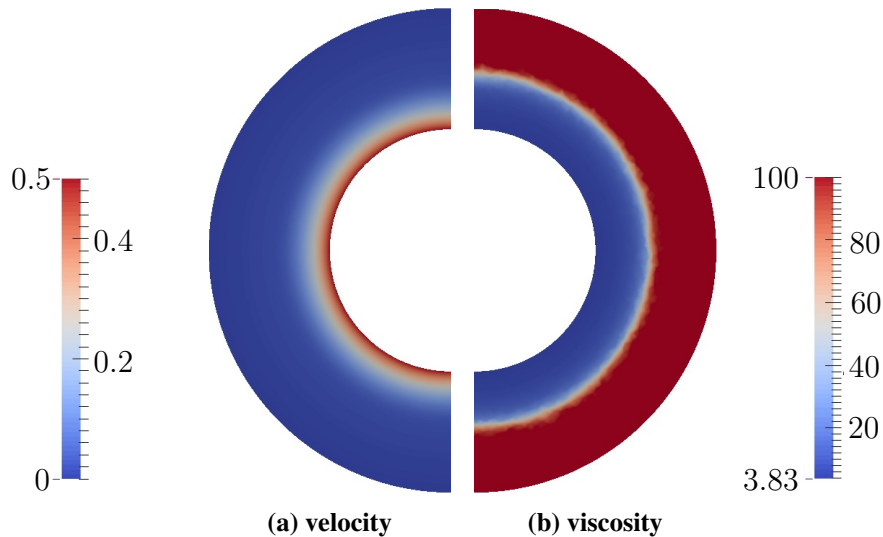


Figure 5: Velocity and viscosity distribution of the benchmark Taylor-Couette flow of a Bingham fluid

outer cylinder wall. After half of the width of the gap the velocity is almost zero. In this zone the shear rate does not reach the threshold and, thus, behaves rigid.

In Fig. 5b the viscosity distribution in the z -plane using the EWC forcing term with backtracking can be seen. At the inner moving wall the velocity is low according to the higher shear rates. The velocity is increasing towards the outer wall until the Newtonian viscosity is reached in the rigid zone.

For the Power Law fluid the nominal viscosity is $\mu_0 = 0.8$, the consistency index $K = 1$ and the power law parameter $n = 0.5$. A Power Law parameter $n < 1$ describes a shear thinning fluid. That means the viscosity is decreasing when the shear rates are increasing. Here, the Reynolds number is $Re = 1.25$.

Figure 6a illustrates the velocity distribution of the Power Law fluid. The velocity decreases continuously from the inner moving wall to the outer fixed wall.

The viscosity distribution of the Power Law fluid is shown in Fig. 6b. In accordance with the velocity and shear rates, the lowest viscosity is at the inner wall, where the highest shear rates can be found. The viscosity is increasing in radial direction towards the outer wall.

To validate our models we compare the analytical solution of the tangential velocity distribution across the gap (Bird et al., 1987; Vola et al., 2004). The velocity profile depends on the viscosity and thus, needs to be evaluated for each rheological model differently. For a Bingham

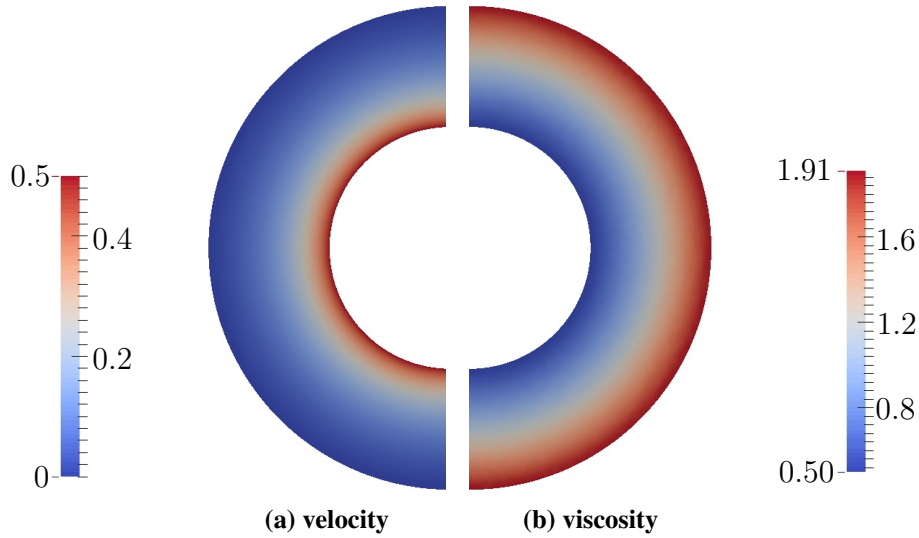


Figure 6: Velocity and viscosity distribution of the benchmark Taylor-Couette flow of a Power Law fluid

fluid the tangential velocity can be calculated as follows:

$$u_r = r \frac{\sqrt{2}\sigma_Y}{4\mu_0} \left(\left(\frac{R_1}{r} \right)^2 - 2\ln \left(\frac{R_1}{r} \right) - 1 \right), \quad (32)$$

where R_i and R_o are the inner and outer radii. R_1 is the transition radius of the rigid zone and can be estimated by solving the following equation:

$$\left(\frac{R_1}{R_i} \right)^2 - 2\ln \left(\frac{R_1}{R_i} \right) - \left(\frac{2\sqrt{2}\mu_0\omega}{\sigma_Y} + 1 \right) = 0 \quad (33)$$

The analytical solution of the tangential velocity for the Power Law fluid can be calculated as follows:

$$u_r = r\omega \left[\left(\frac{R_o}{r} \right)^{\frac{2}{n}} - 1 \right] / \left[\left(\frac{R_o}{R_i} \right)^{\frac{2}{n}} - 1 \right] \quad (34)$$

Figure 7 shows the analytical function of the velocity profile and also the numerical solution. It can be seen that for the Power Law the numerical solution agrees with the analytical. However, the Bingham fluid shows a small deviation that can be seen when the velocity comes closer to zero. In the analytical model the viscosity is assumed to be infinity in the rigid zone and, therefore, has a zero velocity. In the numerical model we assume that the viscosity in the rigid zone is 100 times higher than the Newtonian viscosity. Thus, the velocity decreases but does not get zero.

To still have a validation of the model, the Bingham fluid is simulated using a higher tangential velocity of the inner cylinder, so that the shear rate is always higher than the threshold. For this example the results of the analytical and numerical model matches sufficiently (Fig. 8).

In the following the computational performance of the Taylor-Couette flow is analyzed. Like before we compare characteristic values of the computation performance like the total

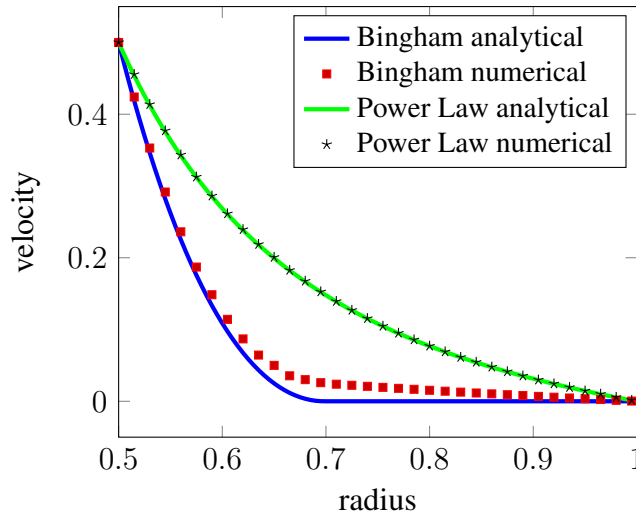


Figure 7: Tangential velocity of the Taylor-Couette flow.

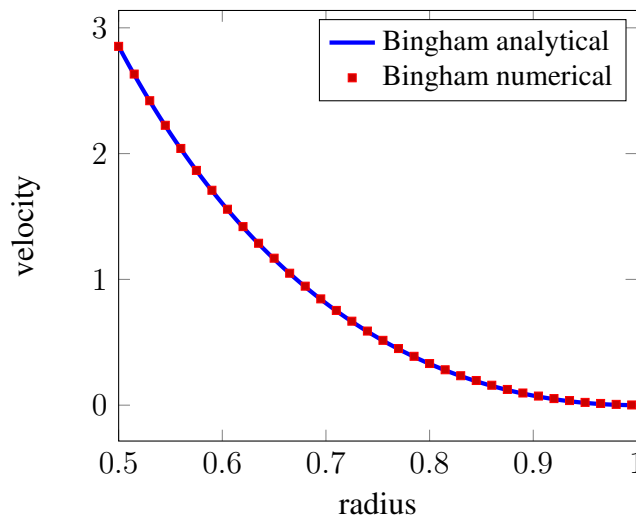


Figure 8: Tangential velocity of the Taylor-Couette flow for the Bingham fluid with a higher velocity.

number of nonlinear iteration steps ($\sum iter$), the number of linear iterations ($\sum NLI$), the line search steps ($\sum LSS$), the line search rejected steps ($\sum LSR$) and the needed CPU time ($CPUtime$).

Table 3 states the characteristic values of the performance of the Taylor-Couette flow simulating of a Bingham fluid of four different forcing terms using backtracking method as globalization strategy. For all cases the total number of nonlinear iteration steps is the same. Also the high numbers of line search rejected steps stand out. Comparing the CPU time the most advantageous forcing term is the EWC with a computation time of 2842 s. The second best option is the GLT forcing term with a CPU time of 2884 s. Regarding the number of iterations the GLT seems to be favorable, which has also the lowest number of line search steps.

The performance of the Taylor-Couette flow of the Power Law fluid of the forcing terms and using backtracking can be seen in Table 4. Here, the EWK forcing term has the lowest CPU time (2167 s) with a total number of nonlinear iteration steps of 5776. The second best performing

Table 3: Performance of the Taylor-Couette flow simulating a Bingham fluid for different forcing terms, with backtracking

Forcing term	$\sum iter$	$\sum NLI$	$\sum LSS$	$\sum LSR$	$CPUtime$
EWC	6400	118948	4802	800	2842
EWK	6400	127952	4807	801	2897
GLT	6400	124988	4800	800	2884
PP	6400	127529	4802	800	2993

forcing term is the GLT with a CPU time of 2180 s. With a total number of nonlinear iteration steps of 5832 the value is slightly higher than the iteration number of the PP forcing term, however, the number of linear iterations is lower. In general the differences of performance for those two forcing terms are small and, therefore, a clear statement cannot be made.

Table 4: Performance of the Taylor-Couette flow simulating a Power Law fluid for different forcing terms, with backtracking

Forcing term	$\sum iter$	$\sum NLI$	$\sum LSS$	$\sum LSR$	$CPUtime$
EWC	5837	71797	0	0	2196
EWK	5776	70244	0	0	2167
GLT	5832	70827	0	0	2180
PP	5809	71005	0	0	2182

Figure 9 and 10 show the tolerance over the time steps. It can be seen that the tolerance is depending on the choice of the forcing term and varies over time.

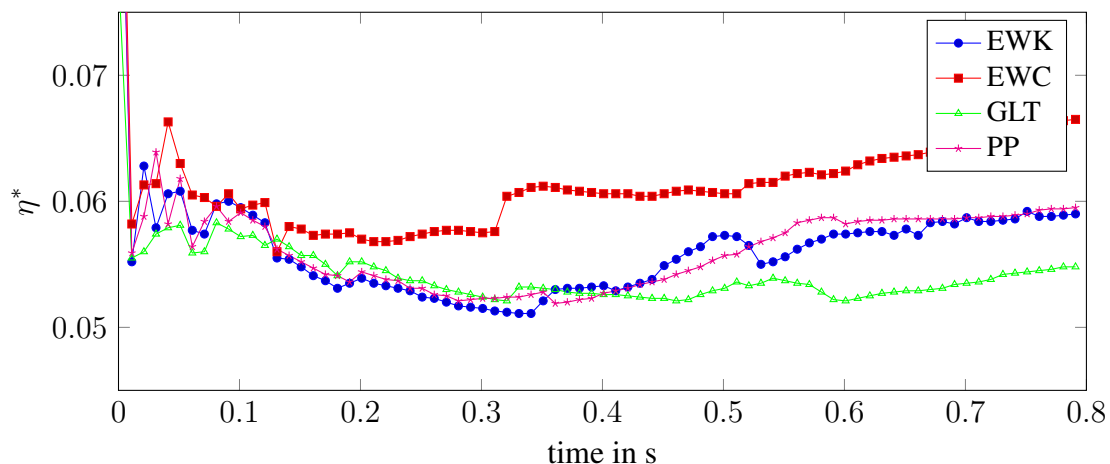


Figure 9: Average forcing term per time step simulating a Bingham fluid of a Taylor-Couette flow

Considering the Bingham fluid for a Taylor-Couette flow the EWC and GLT forcing terms are advantageous. For the Bingham fluid the backtracking method experiences a high number

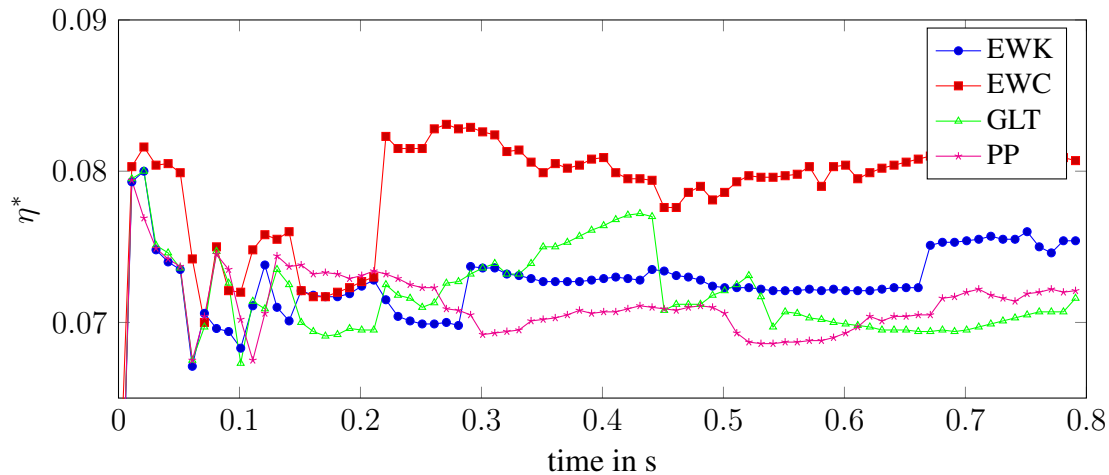


Figure 10: Average forcing term per time step simulating a Power Law fluid of a Taylor-Couette flow

of line search rejected steps, as well as, a high iteration number, can be found. This occurs due to the high nonlinearity of the Bingham fluid.

For the Power Law fluid the EWK and GLT forcing terms are the matter of choice. The Power Law fluid does not cause rejected steps and also needs less computation time compared to the Bingham fluid. The nonlinearities of the Power law are not as distinct as of the Bingham fluid

4 CONCLUSION

Elias et al. (2006a) analyze the performance of inexact Newton methods for non-Newtonian fluids. However, without examining the influence of globalization strategies and forcing terms. We evaluate the performance of the Inexact-Newton Krylov method by simulating non-Newtonian fluid behavior focusing on globalization strategy and several forcing terms. The choice of the forcing term and globalization strategy have a great influence on the performance of the simulation reducing of needed iterations and computing time. The preferable forcing term depends on the geometry, the rheological model and whether the backtracking strategy is used or not.

The GLT forcing term using the backtracking strategy shows the best performance for the benchmark cavity. For simulating a Bingham Fluid of the benchmark Taylor-Couette flow, the EWC forcing term is advantageous. The Power Law fluid of the Taylor-Couette flow shows the best performing results for the EWK forcing term.

Due to the diverse results, it is hard to make a clear statement about a general preferable choice regarding forcing terms simulating non-Newtonian fluid behavior. Thus, the decision on which forcing term should be picked, is to be evaluated according to the actual problem at hand. For our test cases the GLT forcing term showed consequently adequate results using the backtracking method, even though not the best performance. An adaptive time step can lead to a better performance, however, it is also more complex to evaluate. In this study the time step is assumed to be fix for the sake of clarity.

ACKNOWLEDGEMENTS

This work is partially supported by CNPq, FAPERJ, Capes and Petrobras.

REFERENCES

- An, H. B., Mo, Z. Y., & Liu, X. P., 2007. A choice of forcing terms in inexact Newton method. *Journal of Computational and Applied Mathematics*, vol. 200, no. 1, pp. 47.
- Balay, S., Abhyankar, S., Adams, M., Brown, J., Brune, P., Buschelman, K., Dalcin, L., Eijkhout, V., Gropp, W., Karpeyev, D., Kaushik, D., Knepley, M., McInnes, L. C., Rupp, K., Smith, B., Zampini, S., Zhang, H., & Zhang, H., 2016. PETSc Users /manual. Technical Report ANL-95/11 - Revision 3.7, Argonne National Laboratory, 2016.
- Bellavia, S., & Berrone, S., 2007. Globalization strategies for Newton-Krylov methods for stabilized FEM discretization of Navier-Stokes equations. *Journal of Computational Physics*, vol. 226, no. 2, pp. 2317.
- Beverly, C., & Tanner, R., 1992. Numerical analysis of three-dimensional Bingham plastic flow. *Journal of Non-Newtonian Fluid Mechanics*, vol. 42, pp. 85.
- Bird, R., Armstrong, R., & Hassager, O., 1987. *Dynamics of Polymeric Liquids Vol. 1 Fluid Mechanics*. Wiley- Interscience, New York, second ed.
- Bodart, N. L. O., Catabriga, L., & Coutinho, A. L. G. A., 2011. Forcing term effects on the inexact newton-krylov method for solving nonlinear equations emanating from stabilized finite element formulations of navier-stokes equations. *CILAMCE 2011*.
- Crochet, M., Davies, A., & Walters, K., 1984. *Numerical simulation of non-Newtonian flow*. Elsevier, Amsterdam.
- Dembo, R. S., Eisenstat, S. C., & Steihaug, T., 1982. Inexact Newton Methods. *SIAM Journal on Numerical Analysis*, vol. 19, no. 2, pp. 400.
- Dennis Jr., S., & Schnabel, R. B., 1983. *Numerical Methods for Unconstrained Optimization and Nonlinear Equations*. Prentice-Hall.
- Eisenstat, S., & Walker, H., 1996. Choosing the forcing terms in an Inexact Newton method. *SIAM Journal of Scientific Computing*, vol. 17, pp. 16.
- Elias, R., Coutinho, A., & Martins, M., 2004. Inexact-Newton-type methods for non-linear problems arising from the SUPG/PSPG solution of steady incompressible Navier-Stokes equations. *Journal of the Brazilian Society of Mechanical Sciences and Engineering*, vol. 26, pp. 330.
- Elias, R. N., Coutinho, A. L. G. A., & Martins, M. A. D., 2006a. Inexact Newton-type methods for the solution of steady incompressible viscoplastic flows with the SUPG/PSPG finite element formulation. *Computer Methods in Applied Mechanics and Engineering*, vol. 195, no. 23-24, pp. 3145.
- Elias, R. N., Martins, M. A. D., & Coutinho, A. L. G. A., 2006b. Parallel edge-based solution of viscoplastic flows with the SUPG/PSPG formulation. *Computational Mechanics*, vol. 38, no. 4-5, pp. 365.
- Franca, L., & Frey, S., 1992. Stabilized finite element methods: II. The incompressible Navier-Stokes equations. *Computer Methods in Applied Mechanics and Engineering*, vol. 99, pp. 209.

- Gartling, D., 1992. Finite element methods for non-Newtonian flows. Tech. Rep. SAND92-0886, October, CFD Department Sandia National Laboratories, Albuquerque.
- Gomes-Ruggiero, M., Lopes, V., & Toledo-Benavides, J., 2008. A globally convergent inexact Newton method with a new choice for the forcing term. *Annals of Operations Research*, vol. 157, pp. 193.
- Hughes, T., & Tezduyar, T., 1984. Finite element methods for first-order hyperbolic systems with particular emphasis on the compressible Euler equations. *Computer Methods in Applied Mechanics and Engineering*, vol. 45, pp. 217.
- Kelley, C. T., 1995. *Iterative Methods for Linear and Nonlinear Equations*. SIAM.
- Mitsoulis, E., & Zisis, T., 2001. Flow of Bingham plastics in a lid-driven square cavity. *Journal of Non-Newtonian Fluid Mechanics*, vol. 101, pp. 179.
- Owens, R., & Phillips, T., 2002. *Computational rheology*. Imperial College Press.
- Papadrakakis, M., & Balopoulos, V., 1991. Improved quasi-Newton methods for large non-linear problems. *Journal of Engineering Mechanics*, vol. 117, pp. 1201.
- Pawlowski, R., Shadid, J., Simonis, J., & Walker, H., 2006. Globalization techniques for Newton-Krylov methods and applications to the fully coupled solution of the Navier-Stokes equations. *SIAM Review*, vol. 48, pp. 700.
- Rudi, J., Malossi, A. C. I., Isaac, T., Stadler, G., Gurnis, M., Staar, J., P. W., Ineichen, Y., Bekas, C., Curioni, A., Omar, & Ghattas, 2015. An extreme-scale implicit solver for complex pdes: Highly heterogeneous flow in earth's mantle. *In Proceedings of the International Conference for High Performance Computing, Networking, Storage and Analysis*, vol. SC '15, pp. 5:1.
- Tezduyar, T., 1992. Stabilized finite element formulations for incompressible flow computations. *Advances in Applied Mechanics*, vol. 28, pp. 1.
- Tezduyar, T., 1999. Finite elements in fluids: Lecture notes of the short course on finite elements in fluids. *Computational Mechanics Division*, vol. 99-77.
- Tezduyar, T., 2001. Finite element methods for flow problems with moving boundaries and interfaces. *Archives of Computational Methods in Engineering*, vol. 8, pp. 83.
- Tezduyar, T., Aliabadi, S., Behr, M., Johnson, A., Kalro, M., & Litke, M., 1996. Flow simulation and high performance computing. *Computational Mechanics*, vol. 18, pp. 397.
- Tezduyar, T., Mittal, S., & Shih, R., 1991. Time-accurate incompressible flow computations with quadrilateral velocity-pressure elements. *Computer Methods in Applied Mechanics and Engineering*, vol. 87, pp. 363.
- Tezduyar, T. E., & Osawa, Y., 2000. Finite element stabilization parameters computed from element matrices and vectors. *Computer Methods in Applied Mechanics and Engineering*, vol. 190, pp. 411.
- Tuminaro, R., Walker, F., & Shadid, J., 2002. On backtracking failure in Newton-GMRES methods with a demonstration for the Navier-Stokes equations. *Journal of Computational Physics*, vol. 180, pp. 549.

Vola, D., Babik, F., & Latché, J. C., 2004. On a numerical strategy to compute gravity currents of non-Newtonian fluids. *Journal of Computational Physics*, vol. 201, no. 2, pp. 397.

Vola, D., Boscardin, L., & Latché, J., 2003. Laminar unsteady flows of Bingham fluids: a numerical strategy and some benchmark results. *Journal of Computational Physics*, vol. 187, pp. 441.